Molecular Medicine

Prime-Boost Vaccination with rBCG/rAd35 Enhances CD8+ Cytolytic T-Cell Responses in Lesions from *Mycobacterium Tuberculosis*–Infected Primates

Sayma Rahman,[1] Isabelle Magalhaes,[2,3] Jubayer Rahman,[1] Raija K Ahmed,[3] Donata R Sizemore,[4] Charles A Scanga,[4] Frank Weichold,[4] Frank Verreck,[5] Ivanela Kondova,[5] Jerry Sadoff,[4] Rigmor Thorstensson,[3] Mats Spångberg,[3] Mattias Svensson,[1] Jan Andersson,[1,6] Markus Maeurer,[2,3] and Susanna Brighenti[1]

[1]Center for Infectious Medicine, Department of Medicine, Karolinska Institute, Karolinska University Hospital Huddinge, Stockholm, Sweden; [2]Microbiology, Tumor and Cell Biology, Karolinska Institute, Solna, Sweden; [3]The Swedish Institute for Infectious Disease Control, Solna, Sweden; [4]Aeras Global TB Vaccine Foundation, Rockville, Maryland, United States of America; [5]Department of Parasitology, Biomedical Primate Research Centre, Rijswijk, the Netherlands; and [6]Division of Infectious Diseases, Department of Medicine, Karolinska Institute, Karolinska University Hospital Huddinge, Stockholm, Sweden

To prevent the global spread of tuberculosis (TB) infection, a novel vaccine that triggers potent and long-lived immunity is urgently required. A plasmid-based vaccine has been developed to enhance activation of major histocompatibility complex (MHC) class I–restricted CD8+ cytolytic T cells using a recombinant Bacille Calmette-Guérin (rBCG) expressing a pore-forming toxin and the *Mycobacterium tuberculosis* (Mtb) antigens Ag85A, 85B and TB10.4 followed by a booster with a nonreplicating adenovirus 35 (rAd35) vaccine vector encoding the same Mtb antigens. Here, the capacity of the rBCG/rAd35 vaccine to induce protective and biologically relevant $CD8^+$ T-cell responses in a nonhuman primate model of TB was investigated. After prime/boost immunizations and challenge with virulent Mtb in rhesus macaques, quantification of immune responses at the single-cell level in cryopreserved tissue specimen from infected organs was performed using *in situ* computerized image analysis as a technological platform. Significantly elevated levels of $CD3^+$ and $CD8^+$ T cells as well as cells expressing interleukin (IL)-7, perforin and granulysin were found in TB lung lesions and spleen from rBCG/rAd35-vaccinated animals compared with BCG/rAd35-vaccinated or unvaccinated animals. The local increase in $CD8^+$ cytolytic T cells correlated with reduced expression of the Mtb antigen MPT64 and also with prolonged survival after the challenge. Our observations suggest that a protective immune response in rBCG/rAd35-vaccinated nonhuman primates was associated with enhanced MHC class I antigen presentation and activation of CD8+ effector T-cell responses at the local site of infection in Mtb-challenged animals.

Online address: http://www.molmed.org
doi: 10.2119/molmed.2011.00222

INTRODUCTION

The global spread of tuberculosis (TB) continues to be a major threat to public health. The only available TB vaccine, Bacille Calmette-Guérin (BCG), is effective against severe forms of childhood TB but cannot prevent adult pulmonary TB. In general, the efficacy of BCG vaccination is highly variable (0–80%) (1), and the cause of these large differences in vaccine-induced protection is poorly understood. Some of its limitations may involve short-lived BCG-induced immune reactivity and a failure to generate strong major histocompatibility complex (MHC) class I–restricted $CD8^+$ T-cell responses. This underlines the necessity to replace the current BCG vaccine by a more effective vaccine against TB or improve the potency of the already existing BCG.

The immune response to *Mycobacterium tuberculosis* (Mtb) is a dynamic process, and TB control depends on cell-mediated immunity involving polyfunctional $CD4^+$ and $CD8^+$ T-cell responses (2). $CD8^+$ cytolytic T lymphocytes (CTLs) are critical for clearance of intracellular Mtb infection (3), since CTLs trigger target cell and bacterial killing by the coordinated secretion of cytolytic and antimicrobial effector molecules perforin (4) and granulysin (5) into the immunological synapse. Our recent studies on immunopathogenesis in human TB (6,7)

Address correspondence to *Susanna Brighenti, Center for Infectious Medicine, F59, Karolinska University Hospital Huddinge, 141 86 Stockholm, Sweden. Phone: +46-8-58582268; Fax: +46-8-7467637; E-mail: susanna.brighenti@ki.se.*
Submitted June 28, 2011; Accepted for publication February 28, 2012; Epub (www.molmed.org) ahead of print February 29, 2012.

The Feinstein Institute for Medical Research North Shore LIJ

demonstrated an impaired expression of both perforin and granulysin in $CD8^+$ CTLs at the local site of infection in patients with active disease. Furthermore, we found that homeostatic cytokines, such as interleukin (IL)-7 and IL-15, can promote cellular immunity and host protection in experimental TB (8). These observations suggest that a successful TB vaccine should be able to induce potent CTL responses to confer relevant immune protection.

In this study, the immunogenicity and efficacy of a plasmid-based vaccine platform, produced by the Aeras Global TB Vaccine Foundation, was evaluated in a nonhuman primate (NHP) model. Of note, unlike rodent models of TB, outbreed NHPs develop a human-like TB disease and thus provide a more relevant model to study TB-induced immune responses compared with other experimental animals. A heterologous prime-boost approach was used (9), on the basis of a recombinant BCG (rBCG) expressing the Mtb antigens Ag85A, Ag85B and TB10.4 (10). The novel prototype strain rBCG AFRO-1 also has an insertion of a perfringolysin gene (*pfoA*) encoding a mutated pore-forming bacterial cytolysin, which permits leakage of antigens from the phagosome to the cytosolic MHC class I pathway (11). Thus, rBCG may induce a broader and more potent CTL response than parent BCG, which cannot translocate from the phagosomes to access the cytosol (12). Accordingly, it was recently shown that rBCG AFRO-1 enhanced immune responses and prolonged survival compared with parent BCG upon Mtb challenge in mice and guinea pigs (10).

This study is a follow-up of a NHP TB vaccine trail where priming with rBCG AFRO-1 was followed by a boost with AERAS-402, which is a nonreplicating adenovirus 35 vaccine (rAd35) vector also encoding the key Mtb antigens Ag85A, Ag85B and TB10.4 (13). Vaccination with rBCG AFRO-1 and rAd35 AERAS-402 induced strong Mtb-specific T-cell responses in peripheral blood of immunized animals (13). Here, we evaluated the protective efficacy of the rBCG/rAd35 vaccine in tissue biopsies obtained from different organs of animals challenged with virulent Mtb, using a well-established technology on the basis of *in situ* immunohistology and quantitative computerized image analysis (6,7,14–20). Of note, analysis of cells from the peripheral blood requires manipulation *in vitro* and only allows a small proportion of reactive lymphocytes to be monitored (21) but is nevertheless the principal method used to analyze vaccine-induced immune responses. In contrast, *in situ* image analysis provides the opportunity to study the spatial anatomical expression of different proteins and the organ-specific cell–cell interactions in a physiologic environment in which the numbers of pathogen-responder cells are high. Whereas formalin-fixed paraffin-embedded biopsies are often used to study tissue morphology and cellular content, cryopreserved tissue enables quantitative single-cell assessment of cellular and functional effector markers at the local site of infection.

We studied *in vivo* expression and distribution of immune cells and antimicrobial effector molecules in Mtb-infected lung and spleen tissue obtained from rBCG/rAd35- or BCG/rAd35-vaccinated and unvaccinated control NHPs. The functional relationship between immune cells, effector molecules and Mtb-specific antigen load was also investigated in the tissues. Our findings demonstrate that rBCG/rAd35-vaccinated NHPs had a significantly more powerful $CD8\alpha/\beta$ T-cell response than BCG/rAd35-vaccinated and unvaccinated control animals. An elevated level of $CD8^+$ T cells correlated with enhanced IL-7 production and a coordinated expression of perforin and granulysin. Interestingly, two of the rBCG/rAd35-vaccinated animals that demonstrated polyfunctional T-cell responses in peripheral blood after vaccination (13) also produced the most potent $CD8^+$ CTL responses in Mtb-infected tissue. The $CD8^+$ CTL response was particularly enhanced at the site of infection in the pulmonary TB lesions and associated with reduced Mtb-specific antigen load and increased survival of Mtb-infected animals.

MATERIALS AND METHODS

Animals and Vaccine Candidates

Female rhesus macaques (*Macaca mulata*) of Chinese origin (2–3 years old) were housed in a primate center at the Swedish Institute for Infectious Disease Control (Solna, Sweden). Housing and care procedures were in accordance with general guidelines of the Swedish Animal Welfare Agency and approved by the local ethical committee. The priming rBCG vaccine, AFRO-1, was generated from an rBCG strain encoding a mutated perfringolysin O (*pfo*AG137Q) and three mycobacterial antigens: Ag85A, Ag85B and TB10.4 (GenBank accession number P0A4V2, P12942 and AF2122/97, respectively) (10). The booster vaccine, AERAS-402 (rAd35-TBS), was made using a replication-deficient adenovirus serotype 35 encoding a triple fusion of Ag85A, Ag85B and TB10.4 (22).

Immunizations and Mtb Infection

Table 1 shows the study design including immunization schedule (13), Mtb infection and biopsy collection. Briefly, animals were primed with an intradermal injection of either rBCG AFRO-1 or the BCG strain, BCG-SSI 1331, followed by two boosts with intramuscular injections of rAd35 AERAS-402. The booster vaccine was administered to enhance activation of Mtb-specific T cells that were primed by the AFRO-1 vaccine. BCG vaccination was included in the immunization protocol in addition to unvaccinated controls, to validate the results obtained in the rBCG group, but also to study if the booster vaccine would potentially have an effect in combination with parent BCG. Control animals received saline (n = 3) or were untreated (n = 3). Animals were immunized in Sweden and transferred to the Biomedical Primate Research Centre (Rijswijk, the Netherlands) for challenge with virulent Mtb according to ethical approval in both Sweden and the Netherlands. Tissue samples were ob-

tained from all animals during the chronic phase of Mtb infection. Twenty weeks after Mtb challenge, 10 animals were still alive, whereas 8 had been euthanized prematurely at 8–10 wks, after reaching a humane endpoint related to severe pulmonary disease. During necropsy (at humane endpoint or wks 23–24 after infection), multiple tissue samples from pulmonary TB lesions and spleen were collected by an experienced pathologist on the basis of visual examination of the Mtb-infected organs. Biopsies from unaffected lung parenchyma as well as axillary/hilary lymph nodes were also collected from the animals for immunohistochemical analysis *in situ* (Supplementary Figures 1A–J); however, only representative data from lung lesions and spleen are presented here.

Table 1. Study design: immunization schedule, Mtb challenge, survival, and necropsy in the rBCG/rAd35, BCG/rAd35, and control groups.

Number of animals	Prime	Boost 1	Boost 2	Mtb challenge	Survival	Biopsy
6	rBCG AFRO-1	rAd35 AREAS-402	rAd35 AREAS-402	[a]	5	
6	BCG	rAd35 AREAS-402	rAd35 AREAS-402	[a]	2	
6	Saline			[a]	3	
Timeline in weeks	0 ↓	15 ↓	27 ↓	39 ↓	59 ↓	62–63 ↓ Necropsy

[a]500 CFU Mtb Erdman by intratracheal instillation.

Colony-Forming Units

Lung tissue was collected and cryopreserved at –80ºC for determination of bacterial load. After thawing, the lung tissue was minced to enable random sampling for further tissue homogenization. Fully processed lung tissue samples were serially diluted and plated on supplemented Middlebrook 7H10 (Tritium Microbiologie, Veldhoven, the Netherlands), and colony-forming units (CFUs) were counted 3–5 wks later. Mycobacterial burden was calculated as $\log_{10}$CFU per gram of lung tissue.

Immunohistochemistry of Frozen Tissue Sections

Frozen tissue biopsies obtained from Mtb-infected organs were embedded in Cryo-OCT-compound (Sakura Tissue-TEK, Torrance, CA, USA) before cryosectioning (8 μm) and fixation in 4% formaldehyde (Sigma-Aldrich, St. Louis, MO, USA). Tissue sections were incubated with primary antibodies overnight at room temperature and blocked with normal serum before incubation with secondary antibodies at room temperature for 30 min. Tissues stained with secondary antibodies alone or appropriate isotype controls were used as negative controls. Immunohistochemistry was performed according to the standard avidin-biotin complex (ABC) method (15), and positive staining was developed using a diaminobenzidine substrate (Vector Laboratories, Burlingame, CA, USA) and hematoxylin for nuclear counterstaining. Two-color staining was performed using indirect immunofluorescence and confocal microscopy (Leica TCS SP2 AOBS; Leica Microsystems and Leica Imaging Systems, Wetzlar, Germany).

In Situ Computerized Image Analysis

Protein expression was quantified at the single-cell level (14) using a DMR-X microscope and a digital image analysis system (Quantimet Q5501W) including the highly sensitive Qwin 550 software (Leica Microsystems and Leica Imaging Systems) according to the following procedure (Figure 1): (a) perform digital exclusion of tissue artifacts and highly necrotic areas; (b) set the threshold for the intensity of positive staining (green contour line in Figure 1); (c) set the threshold for the total cell area by including both positive (diaminobenzidine) and negative staining (hematoxylin) (red/orange contour line in Figure 1); (d) determine protein expression of a specific marker as the percentage of positively stained area within the total cell area; and (e) use determined threshold value to scan tissue sections (that is, 10–40 high-power fields/tissue section). The mean value of the protein expression in the tissue is presented at the end of the analysis. The Qwin software can detect and separate 16.7 million different colors, which enable sensitive quantification of positive staining and can easily exclude potential background staining from the analysis. This is a well-established quantitative method that has been extensively used primarily in humans (6,7,14–18) and NHPs (19,20) for analysis of a wide range of proteins (that is, cell surface proteins; cytoplasmic, granule-associated or nuclear proteins; secreted proteins; and so on) to describe the phenotype and function of different cell types present in tissue.

Antibodies

Primary antibodies were monoclonal antibodies directed against human antigens (cross-reactive with NHPs): CD3 and CD68 (DAKO, Glostrup, Denmark), CD4 (Biocare Medical, Walnut Creek, CA, USA), CD8α (BD Biosciences, Franklin Lakes, NJ, USA), CD8β (2ST8.5H7; Beckman Coulter, Brea, CA, USA), CD20 (Abcam, Cambridge, UK), perforin (Pf16-17; Mabtech, Stockholm, Sweden) and IL-7 (B-N18; Diaclone, Besancon, France). Expression levels of total $CD8^+$ T cells ($CD8\alpha\alpha^+$ and $CD8\alpha\beta^+$) and $CD8\alpha\beta^+$ T cells ($CD8\beta^+$) were determined in the tissue. Affinity-purified rabbit polyclonal antibodies against granulysin or the secreted Mtb-specific protein, MPT64, were provided by Professors Alan Krensky and Carol Clayberger (Stanford University, Stanford, CA, USA) and also Professors Harald Wiker and Lisbet Sviland (Bergen University, Norway), respectively. Biotiny-

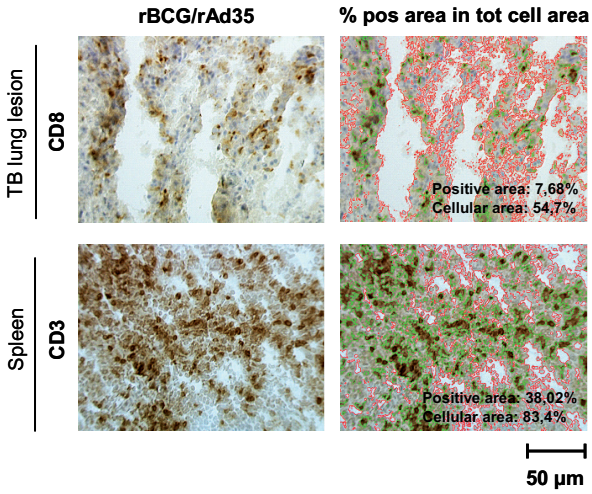

Figure 1. Protein expression in NHP lung and spleen tissue was quantified using *in situ* computerized image analysis of immunohistochemistry data. Immunohistochemistry images (left panel) illustrate positive immunostaining for CD8α+ T cells or CD3+ T cells (brown) in Mtb-infected tissue obtained from an rBCG/rAd35-vaccinated animal. The threshold values for the positive staining (green contour line) and the total cell area (red/orange contour line), illustrated in the overlay image (right panel), was set using a digital image analysis system including a highly sensitive Qwin 550 software. The data are presented in field statistics as the total area measured, intensity, positive area and cellular area. A mean value of the percent positive area of the total cell area in the tissue was quantified in 10–40 high-power fields and plotted in separate graphs. Magnification 125×.

lated goat anti-mouse IgG and swine anti-rabbit F(ab')$_2$ were purchased from DAKO. For dual staining, spleen tissue was stained with rat anti-human CD8 or CD4 (Serotec, Oxford, UK) and mouse anti-human perforin followed by the appropriate Alexa Fluor–conjugated secondary antibody (Molecular Probes, Eugene, OR, USA).

IL-7 Stimulation of Peripheral Blood Mononuclear Cells *In Vitro*

Frozen peripheral mononuclear cells (PBMCs) from three healthy NHPs were thawed, rested overnight and incubated for 6 h in AIM-V medium (Gibco; Invitrogen, Grand Island, NY, USA) containing 10 µg/mL brefeldin A (BFA) (Sigma-Aldrich) and 1 µg/mL BD GolgiStop™ (BD Biosciences) in the presence or absence (negative control) of 100 ng/mL recombinant IL-7 (R&D Systems). PBMCs incubated with plate-bound anti-CD3 (SP34; Invitrogen) and anti-CD28 (CD28.2; Beckman Coulter) antibodies were used as a positive control. Flow cytometric analysis (Gallios flow cytometer with Kaluza software; Beckman Coulter; Supplementary data, Figure 2A) was performed using anti-CD3 Pacific Blue (SP34-2), anti-CD4 PerCP-Cy5.5 (L200) and anti-CD8α APC-Cy7 (SK1) antibodies (BD Biosciences) and intracellular staining for perforin (Pf-344 FITC; Mabtech) using the IntraPrep Fix/Perm Kit (Beckman Coulter).

Statistical Analysis

Because of the small sample size in each group, the data are presented as median ± interquartile range (IQR) in bar graphs (n = 5–6) or scatter dot plots (n = 8–10). A nonparametric Kruskal-Wallis test was used to calculate statistical significance. The statistical significance was determined as follows: $^{*}P < 0.05$, $^{**}P < 0.01$, $^{***}P < 0.0001$. $P > 0.05$ was considered nonsignificant. A nonparametric Spearman correlation test was used for the correlation analysis (n = 16–17). All statistical analyses were performed using Graph Pad Prism-4.

All supplementary materials are available online at www.molmed.org.

RESULTS

Reduced Expression of Collagen Type I and Mtb-Specific Antigen MPT64 in Pulmonary TB Lesions and Spleen of rBCG/rAd35-Vaccinated Animals

Quantitative *in situ* computerized image analysis (see Figure 1) was used to measure the expression levels of different proteins in cryopreserved tissue biopsies from pulmonary TB lesions and spleen obtained from rBCG/rAd35-vaccinated, BCG/rAd35-vaccinated and unvaccinated animals after Mtb infection. In general, the cellularity of pulmonary tissue was significantly more spacious compared with the compact lymphoid structure of the spleen (see Figure 1). As illustrated in Figure 2, fibrosis and necrotic TB granuloma formation including giant cells (GCs) were more frequently observed among BCG/rAd35-vaccinated and unvaccinated control animals compared with the rBCG/rAd35 vaccine group (Figure 2A). Accordingly, collagen type I, which is commonly associated with fibrosis as a result of extensive necrosis and scar formation in chronic diseases including TB (23), was significantly lower ($P < 0.01$) in the rBCG/rAd35-vaccinated primates compared with the controls (Figure 2C). In addition, there was a general tendency (nonsignificant) toward lower cellularity in the lung lesions of rBCG/rAd35-vaccinated animals (Figure 2A) that may suggest a lower level of pathological inflammation compared with the other groups (6).

On average, the bacterial load in the lungs of Mtb-infected animals that survived until the end of the study was lower compared with the animals that died during the course of the study (manuscript in preparation). The highest CFU counts were found in the unvaccinated controls with a group median of 5.32 $\log_{10}$CFU/g (range 4.59–6.85), whereas both vaccine groups showed a reduction in bacterial load in

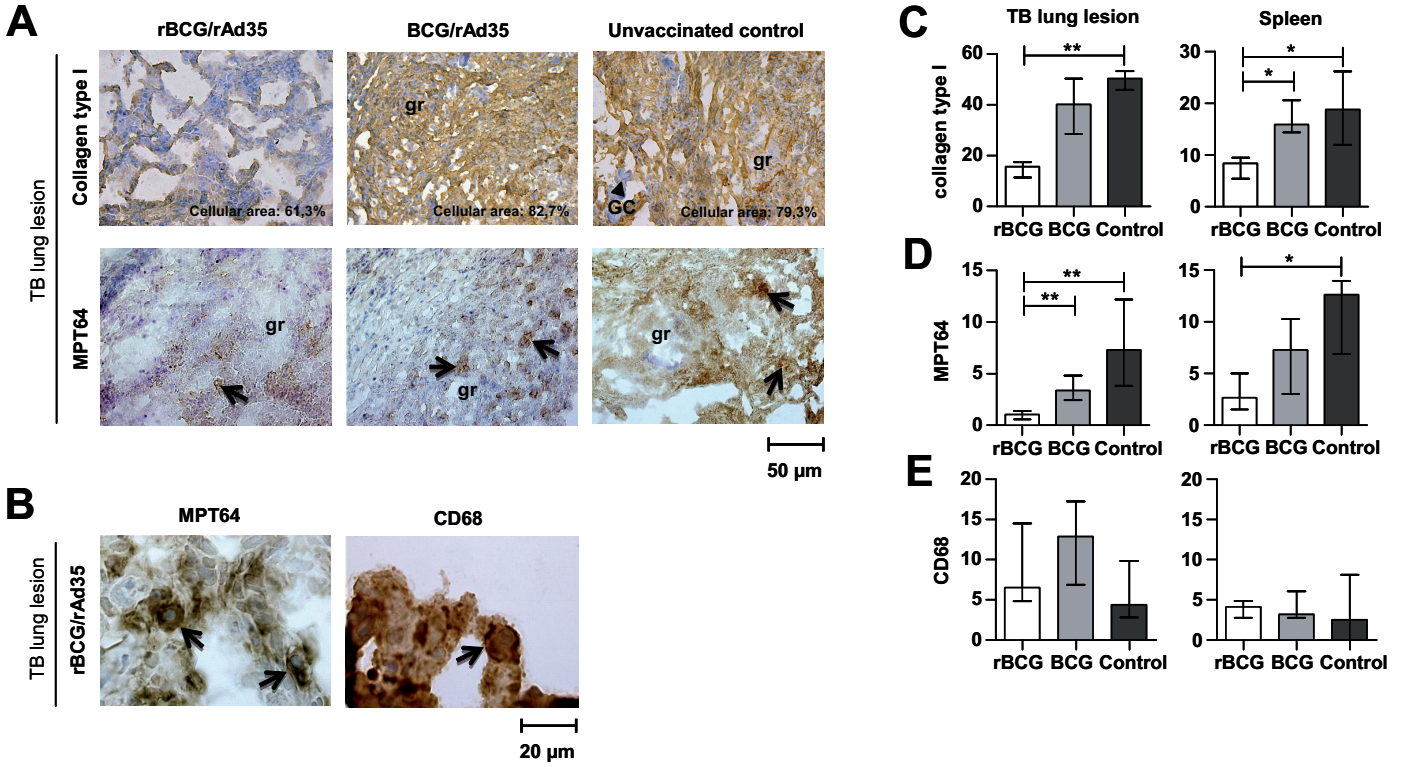

Figure 2. Vaccination with rBCG/rAd35 resulted in reduced collagen type I deposition as well as reduced Mtb-specific antigen load in lung and spleen from Mtb-infected animals. (A) Representative immunohistochemical images demonstrate expression and distribution of collagen type I (upper panel) and the Mtb-specific antigen MPT64 (lower panel) in pulmonary TB lesions obtained from the rBCG/rAd35 and BCG/rAd35 vaccine groups as well as the unvaccinated control. Granulomatous areas (gr) with the presence of characteristic giant cells (GC; arrowheads) are shown in the TB lesions. Arrows indicate positive cells (brown), whereas negative cells (blue) were counterstained with hematoxylin. Granulomatous lung tissue contained high levels of collagen type I and MPT64. The median cellularity obtained in the collagen type I staining is also shown in the upper panel. Magnification 125×. (B) The higher-magnification image (600×) reveals cytoplasmic expression of MPT64 and CD68 in cells present in the granulomatous area of a pulmonary TB lesion from an rBCG/rAd35-vaccinated animal. *In situ* computerized image analysis of collagen type I (C), MPT64 (D) and CD68 (E) expression in TB lung lesion and spleen tissue of rBCG (rBCG/rAd35) or BCG (BCG/rAd35) vaccinated and control (unvaccinated) animals is shown. Data are presented as percent positive area of the total cell area, and the median ± IQR from n = 5–6 animals/group is shown. Statistical significance of differences in protein expression was determined by a nonparametric Kruskal-Wallis test. *$P < 0.05$, **$P < 0.01$.

the lung. The reduction in the rBCG/rAd35 vaccine group was 0.52 (range 4.44–5.12; $P = 0.11$), whereas the decrease in the BCG/rAd35 vaccine group was 0.72 $\log_{10}$CFU/g (range 3.87–5.66; $P = 0.093$). Here, the expression of the Mtb-specific protein MPT64 (24), which is only secreted by actively dividing bacteria (25), was assessed to determine antigen load in the Mtb-infected tissue. Although immunostaining for the MPT64 antigen was mostly confined to the granulomas, MPT64$^+$ cells could also be detected in non-granulomatous areas of the infected tissue (see Figure 2A). MPT64$^+$ cells and CD68$^+$ alveolar macrophages are also shown at a higher magnification in Figure 2B. *In situ* computerized image analysis was used to quantify the MPT64 staining and demonstrated a significantly ($P < 0.01$) reduced antigen load in pulmonary TB lesions and spleen of rBCG/rAd35-vaccinated compared with BCG/rAd35-vaccinated and control animals (Figure 2D), whereas the proportion of CD68$^+$ macrophages was comparable in all three groups (Figure 2E). Although the bacterial loads in the Mtb-infected lungs were similar between rBCG/rAd35- and BCG/rAd35-vaccinated primates, the significantly lower levels of the MPT64 secretory protein in the TB lesions from the rBCG/rAd35 vaccine group may suggest a different metabolic state of the bacteria in these animals (25).

Increased Proportions of Lymphocyte Subsets in Pulmonary TB Lesions and Spleen of rBCG/rAd35-Vaccinated Animals

Next, we investigated whether rBCG/rAd35-vaccinated animals exhibited a different immune cell profile in

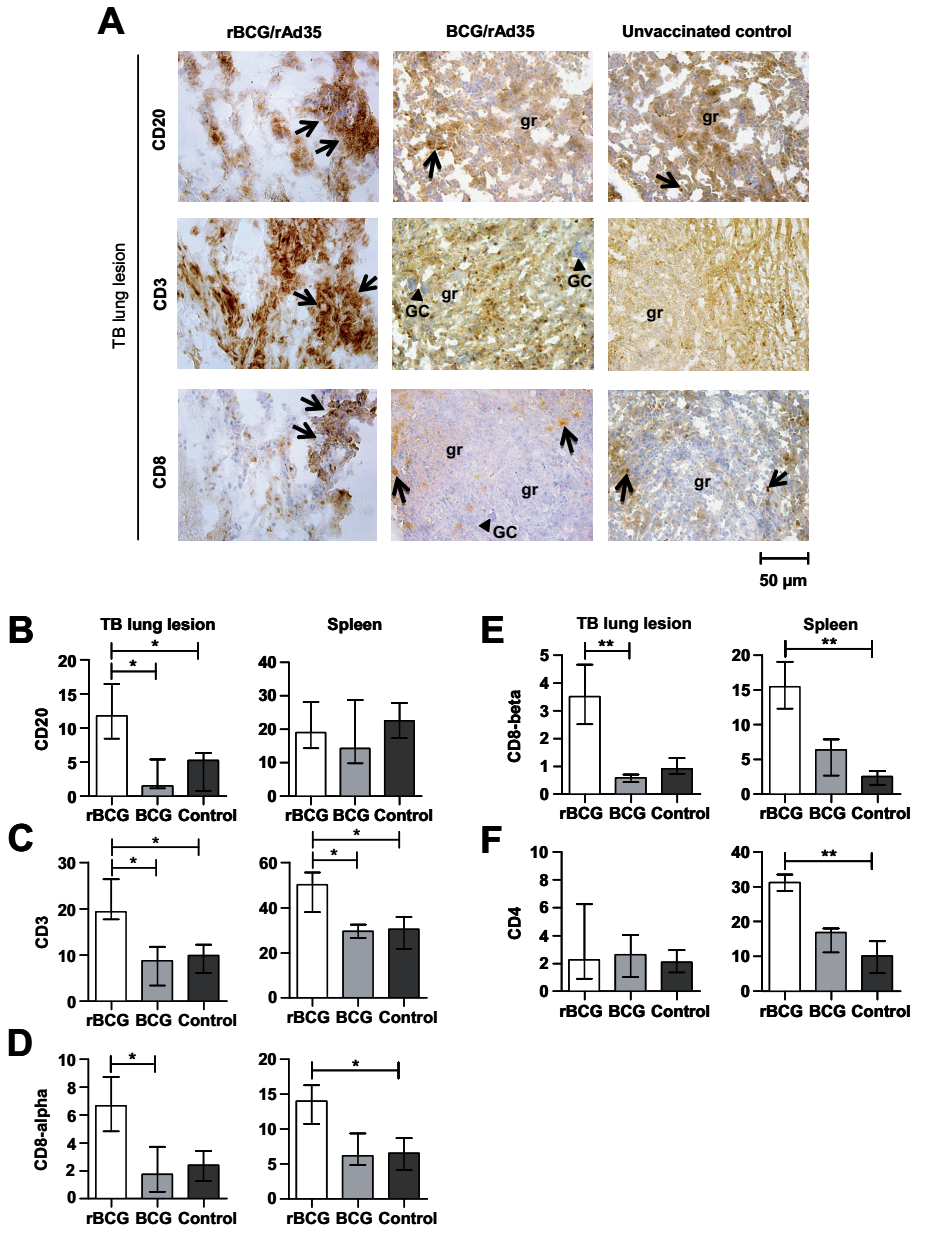

Figure 3. Vaccination with rBCG/rAd35 resulted in elevated levels of different lymphocyte populations in lung and spleen from Mtb-infected animals. (A) Microscopic images of $CD20^+$ B cells (upper panel) and $CD3^+$ (middle panel) and CD8α T cells (lower panel) in TB lung lesions from the rBCG/rAd35 and BCG/rAd35 vaccine groups as well as the unvaccinated control. Immunohistochemical staining was performed, and granulomatous areas (gr) with the presence of characteristic giant cells (GC; arrowheads) are shown in the TB lesions. Arrows indicate positive cells and cell infiltrates (brown), whereas negative cells (blue) are counterstained with hematoxylin. Magnification 125×. Protein expression of $CD20^+$ B cells (B), $CD3^+$ T cells (C), $CD8\alpha^+$ T cells (D), $CD8\beta^+$ T cells (E), and $CD4^+$ T cells (F) was assessed using computerized image analysis to determine the median protein expression (± IQR) in lung lesions and spleen tissues among rBCG (rBCG/rAd35) or BCG (BCG/rAd35) vaccinated and control (unvaccinated) animals. The data from n = 5–6 animals/group are presented as percent positive area of the total cell area. Statistical significance of differences in protein expression was determined by a nonparametric Kruskal-Wallis test. $^*P < 0.05$, $^{**}P < 0.01$.

lung and spleen after an Mtb challenge compared with BCG/rAd35-vaccinated and control animals. We were able to demonstrate abundant expression of $CD20^+$ B cells, $CD3^+$ T cells and $CD8\alpha^+$ T cells in pulmonary TB lesions and spleen after rBCG/rAd35 vaccination (Figure 3). Of note, the different lymphocyte subsets were mostly localized in inflammatory infiltrates in the lung lesions of rBCG/rAd35-vaccinated NHPs (Figure 3A, arrows). Instead, relatively lower numbers of lymphocytes were mainly confined to the peripheral areas of the pulmonary granulomas in the BCG/rAd35-vaccinated and unvaccinated group (see Figure 3A). Quantitative computerized image analysis revealed a significant ($P < 0.05$) increase in $CD20^+$ B cells in rBCG/rAd35-vaccinated lungs (Figure 3B), whereas $CD3^+$ T cell levels were significantly higher ($P < 0.05$) in both lung and spleen (Figure 3C) of rBCG/rAd35-vaccinated animals compared with BCG/rAd35-vaccinated or control animals. Levels of $CD8\alpha^+$ T cells were particularly ($P < 0.05$) elevated at the site of infection in rBCG/rAd35-vaccinated lungs, whereas a significant ($P < 0.01$) increase in the number of $CD8\beta^+$ T cells was evident in both lung lesions and spleens of the rBCG/rAd35-vaccinated animals compared with the BCG/rAd35 vaccine and control groups (Figures 3D–E). However, $CD4^+$ T-cell numbers were significantly increased ($P < 0.001$) in spleen but not lung of the rBCG/rAd35 vaccine group compared with the controls (Figure 3F), demonstrating a relatively increased proportion of $CD8^+$ T cells at the site of infection. Accordingly, the ratio of $CD8^+$ to $CD4^+$ T cells was considerably higher in TB lung lesions (3:1; 6.7% versus 2.2%) than in spleen tissue (1:2; 13.9% versus 31.2%) of rBCG/rAd35-vaccinated animals. Because T cells are a major cell type in lymphoid tissues, a relatively higher proportion of $CD3^+$ T cells in rBCG/rAd35-vaccinated spleen could be partly explained by enhanced granuloma formation and elevated levels of fibrosis

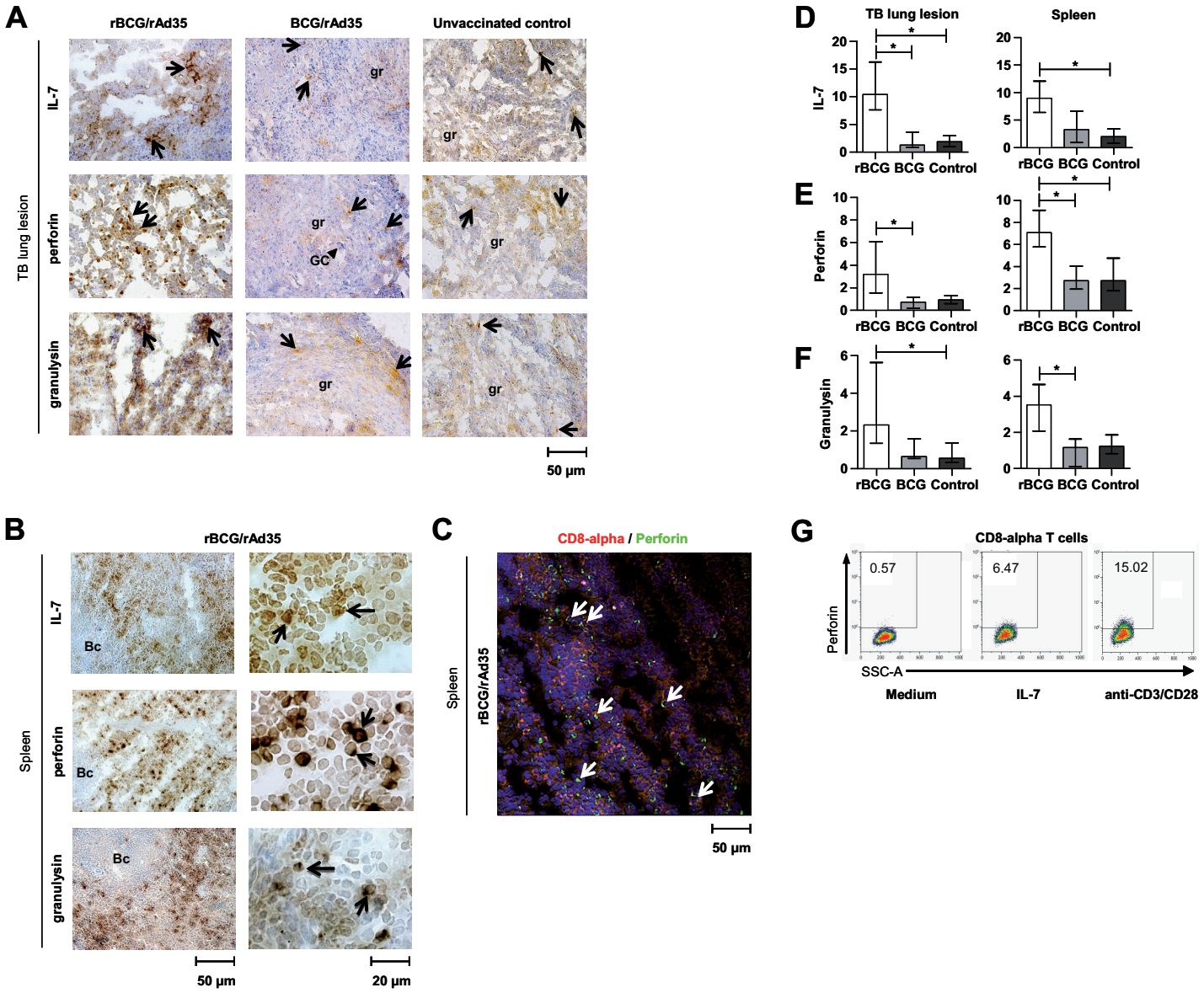

Figure 4. Vaccination with rBCG/rAd35 resulted in induction of IL-7 as well as perforin and granulysin protein in lung and spleen from Mtb-infected animals. (A) Representative immunohistochemical images illustrate IL-7 (upper panel), perforin (middle panel) and granulysin (lower panel) expression in TB lung lesions from the rBCG/rAd35 and BCG/rAd35 vaccine groups as well as the unvaccinated control. Granulomatous areas (gr) with the presence of characteristic giant cells (GC; arrowheads) are shown in the TB lesions. Arrows indicate positive cells (brown), whereas negative cells (blue) were counterstained with hematoxylin. The expression of IL-7, perforin and granulysin were very low in the granulomatous areas. Magnification 125×. (B) Images of IL-7, perforin and granulysin expression in spleen from an rBCG/rAd35-vaccinated animal. These proteins were rarely found in the B-cell areas (Bc) of the spleen. Magnification 125×. Higher magnification (600×) shows cell-associated (high-intensity) and extracellular (low-intensity) expression of IL-7 in splenocytes as well as granular and polarized expression of granule-associated effector molecules in splenic lymphocytes. (C) Two-color staining demonstrates high colocalization of perforin (green; Alexa-488) and $CD8^+$ T cells (red; Alexa-594) in spleen tissue. White arrows indicate double-positive cells. *In situ* computerized image analysis was used to assess the median expression (± IQR) of IL-7 (D), perforin (E) and granulysin protein (F) in lung lesions and spleen tissues among the different groups as indicated. The results from n = 5–6 animals/group are presented as percent positive area of the total cell area, and statistical significance of differences in protein expression was determined by a nonparametric Kruskal-Wallis test. (G) The frequency of perforin-positive cells among $CD8^+$ T cells was detected by flow cytometric analysis after *in vitro* IL-7 short-term stimulation of PBMCs from NHPs for 6 h. Representative data from one of three animals are shown. *$P < 0.05$.

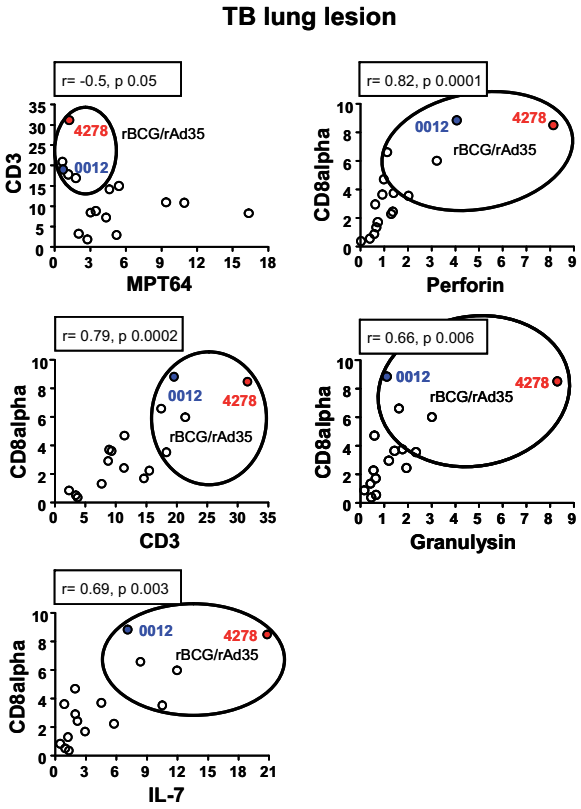

Figure 5. Low levels of Mtb-specific antigen MPT64 correlates with an elevated proportion of $CD3^+/CD8^+$ T cells and enhanced cytolytic T-cell responses in TB lung lesions from Mtb-infected animals. Correlation analyses were performed to assess the associations between the following: Mtb antigen load (MPT64) and $CD3^+$ T cells; $CD3^+$ T cells and $CD8^+$ T cells; and $CD8^+$ T cells and IL-7, perforin or granulysin in the lung tissue of Mtb-infected animals. Data from animals in the rBCG/rAd35-vaccinated group are encircled in the graphs. In addition, data from two animals in the rBCG/rAd35-vaccinated group that presented polyfunctional T-cell responses in blood (13) are given in red (ID 4278) and blue (ID 0012) symbols. In the correlation graphs, data from individual animals (n = 16) are presented as percent positive area of total cell area, and the correlation between indicated markers were determined using Spearman's correlation test. A value of $r = 1$ for the correlation coefficient (r_s) indicates a perfect correlation, whereas $r = -1$ indicates a perfect negative or inverse correlation.

and necrosis in parent BCG/rAd35-vaccinated and control animals, as illustrated in Figures 2A and C.

Induction of IL-7 and Antimicrobial Effector Molecules in Pulmonary TB Lesions and Spleen of rBCG/rAd35-Vaccinated Animals

In situ expression and distribution of IL-7 as well as the antimicrobial effector molecules perforin and granulysin in TB lung lesions obtained from rBCG/rAd35-vaccinated animals compared with BCG/rAd35-vaccinated and control NHPs is shown in Figure 4A. Similar to the expression of $CD3^+$ and $CD8^+$ T cells (Figure 3A), perforin and granulysin were mostly confined to the inflammatory infiltrates in the rBCG/rAd35-vaccinated group but to the periphery of pulmonary granulomas in the BCG/rAd35 and the unvaccinated group (Figure 4A). Distribution and intracellular expression of IL-7, perforin and granulysin in spleen from the rBCG/rAd35 vaccine group is also illustrated in Figure 4B. IL-7 is mainly produced by stromal cells, whereas human monocytes could also express IL-7 upon mycobacterial infection (26). A typical cytoplasmic granular and polarized expression pattern of both perforin and granulysin was detected in cells with a distribution (see Figures 4A, B) and morphology (see Figure 4B) consistent with small activated T lymphocytes. Of note, most cells expressing IL-7 or the antimicrobial effector molecules were located in the T cell–rich areas outside the B-cell follicles found in spleen tissue (see Figure 4B). Accordingly, most perforin-expressing cells in spleen tissue were localized together with CD8α staining (Figure 4C). *In situ* image analysis revealed that protein levels of IL-7 and the granule-associated effector molecules were significantly ($P < 0.05$) elevated in both lung and spleen tissue from rBCG/rAd35-vaccinated animals compared with BCG/rAd35-vaccinated and unvaccinated control animals (Figures 4D–F). Interestingly, *in vitro* IL-7 stimulation of PBMCs obtained from healthy NHPs induced a minor population of perforin-positive cells among $CD8^+$ T cells (Figure 4G) but not in $CD4^+$ T cells (data not shown).

Reduced MPT64 Antigen Load in TB Lung Lesions and Spleen Correlated With Enhanced $CD8^+$ CTL Responses in rBCG/rAd35-Vaccinated Animals

We performed correlation analyses to study the functional relationship between Mtb antigen, T cells and antimicrobial effector molecules in Mtb-infected tissue. Because statistically similar results were obtained from TB lung lesions and spleen, representative data from lung are shown in Figure 5. An inverse correlation was found between MPT64 antigen load and $CD3^+$ T cells in TB lung lesions (Figure 5). Conversely, there was a significant positive correlation between $CD3^+$ and $CD8^+$ (see Figure 5) but not $CD3^+$ and $CD4^+$ T cells (data not shown). Similarly, the association between IL-7 and $CD8^+$ but not $CD4^+$ T cells was highly significant at both tissue sites. An enhanced proportion of $CD8^+$ T cells in

Mtb-infected tissue also correlated with a coordinated expression of perforin and granulysin (see Figure 5). However, there was no significant association between $CD4^+$ T cells and either perforin or granulysin (data not shown).

Previously, two individual NHPs (animal ID 4278 and ID 0012) were shown to exhibit Ag85A/B-specific polyfunctional (coexpression of IL-2, interferon [IFN]-γ and tumor necrosis factor [TNF]-α) T-cell responses in peripheral blood 1 wk after the first Mtb-antigen boost (13). Examination of the immune response induced in the rBCG/rAd35-vaccinated group (see Figure 5, encircled symbols) and particularly in these two animals (red [ID 4278] and blue [ID 0012] symbols, respectively) demonstrated that these animals presented the highest proportions of $CD3^+$ and $CD8^+$ T cells as well as IL-7 and antimicrobial effector molecules, which correlated with the lowest levels of MPT64 antigen in the infected lung (see Figure 5) and spleen tissue (data not shown). The rBCG/rAd35-vaccinated animal ID 4278 also demonstrated higher TB10.4-specific Th1 cytokine responses 15 wks after Mtb infection compared with a BCG-primed animal (Supplementary Table 1 and Figure 2B). Altogether, these observations support the hypothesis that polyfunctional T-cell responses in the circulation were involved in priming CTL responses at the site of Mtb infection.

Survival of Mtb-Infected Animals Is Associated With Decreased MPT64 Antigen Expression and Elevated $CD8^+$ CTL Responses in TB Lung Lesions

We also investigated the immune response induced among rBCG/rAd35-vaccinated (red symbols) and BCG/rAd35-vaccinated (blue symbols) animals as well as unvaccinated (green symbols) Mtb-infected animals that survived until the end of the study (S = survival group) compared with animals that died during the course of the study (D = deceased group) (Figure 6). The survival group had significantly lower expression of the MTP64 antigen and CD68 in the lung, whereas expression of all other cells and effectors, apart from CD4, was significantly elevated compared with the deceased group. The only markers that were significantly changed in the spleen were CD68 and CD3. Of note, the only deceased animal in the rBCG/rAd35 vaccine group had a reduced expression of total CD3 T cells as well as perforin and granulysin in the lung. These results support the findings that survival of Mtb-infected animals requires perforin and granulysin expressing T cells, particularly at the site of infection in pulmonary tissue.

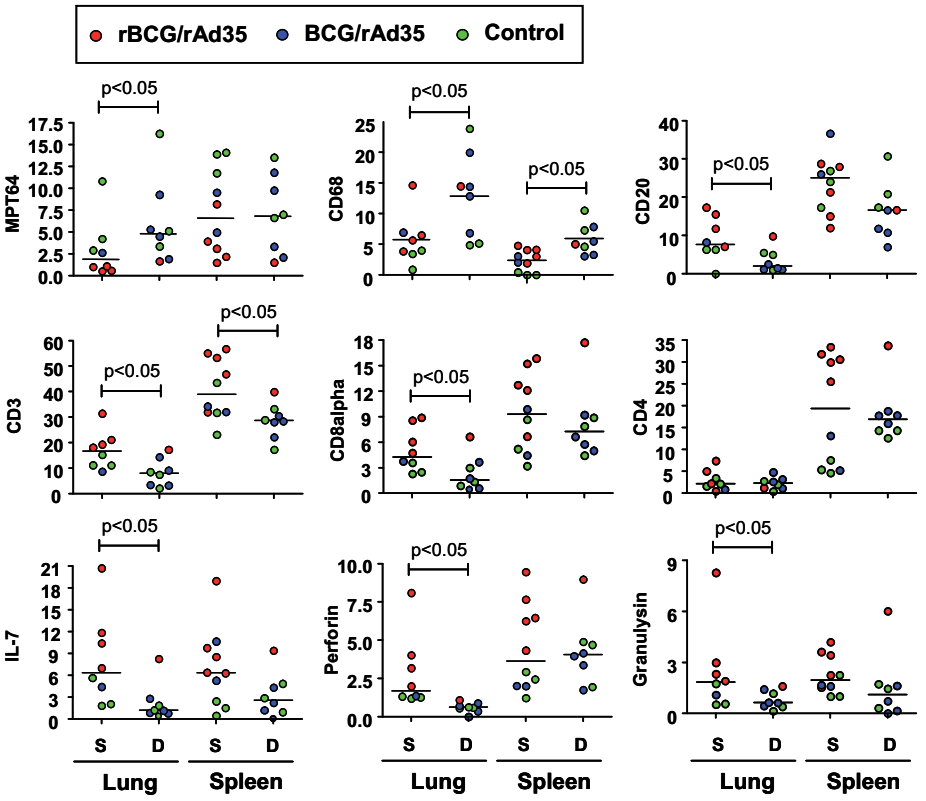

Figure 6. Survival of Mtb-infected animals was associated with enhanced $CD8^+$ CTL responses and reduced Mtb antigen load, particularly at the site of infection in the lung. Immune responses induced in TB lung lesion and spleen of the S = survival group as compared with the D = deceased group. The different prime-boost regimens are indicated in red (rBCG/rAd35), blue (BCG/rAd35) and green (unvaccinated control) symbols. Animals in the survival group (n = 10) remained alive until the end of the trial (wks 23–24), whereas animals in the deceased group (n = 8) died from their TB disease during the course of the trial (wks 10–18). Lung biopsies from one rBCG/rAd35- and one BCG/rAd35-vaccinated NHP are missing and thus the number of animals in the survival group is lower in lung compared with spleen. The median protein expression of Mtb antigen (MPT64), immune cells (CD68, CD20, CD3, CD8 and CD4) and effector molecules (IL-7, perforin and granulysin) are presented as percent positive area of the total cell area. Statistical significance of differences in protein expression was determined by a nonparametric Kruskal-Wallis test.

DISCUSSION

A new TB vaccine with the ability to prime potent multifunctional T-cell responses is urgently required to limit the global spread of TB. In this study, an NHP model and a prime-boost regimen was used to explore the nature of the cellular immune response induced upon vaccination with a new TB vaccine prototype strain, rBCG AFRO-1, followed by a boost with rAd35 AERAS-402, compared with parent BCG/rAd35-vaccinated animals and unvaccinated controls. Our re-

sults from quantitative *in situ* image analysis in lung and spleen tissue demonstrated that immune protection and reduced tissue expression of Mtb-specific antigens correlated with an increased proportion of $CD8^+$ T cells and a highly coordinated expression of the antimicrobial effector molecules perforin and granulysin. Significantly enhanced CTL responses in the rBCG/rAd35-vaccinated animals were strongly associated with elevated levels of IL-7 protein *in situ*, and recombinant IL-7 could induce perforin expression in $CD8^+$ T cells *in vitro*. These results suggest that the rBCG/rAd35 vaccine enhanced MHC class I antigen presentation and subsequent activation of $CD8^+$ CTLs, especially at the site of infection in pulmonary TB lesions but also in the lymphoid compartments.

In chronic infections such as TB, it is of significant relevance to study representative T-cell responses in the infected tissue, since most Mtb-specific T cells accumulate at the site of infection (27–31). We found that lymphocytes were mostly organized in inflammatory infiltrates in the Mtb-infected lung, and, accordingly, perforin- as well as granulysin-expressing cells were defined to the parafollicular areas of the spleen. Of note, we have previously used tissue-based image analysis to show that active TB infection in humans is associated with reduced $CD8^+$ CTLs and impaired expression of antimicrobial molecules in granulomatous lesions (6,7). Similarly, we applied *in situ* technology to demonstrate that the CTL response in Mtb-infected NHPs was significantly enhanced by immunization with the novel rBCG/rAd35 vaccine construct. The information acquired from quantitative *in situ* analysis provides important insights into the host–microbe interplay at the site of infection, in the context of a physiologically relevant milieu that is difficult to reproduce in cell culture models. Moreover, vaccine-induced T-cell responses detected in the peripheral circulation may be different in blood compared with the disease sites (32,33), which underlines the importance to use complementary methods to assess systemic and local immune responses.

Polyfunctional Th1 cells, simultaneously producing IFN-γ, IL-2 and TNF-α, have been used to assess vaccine-mediated protection against intracellular infections (34) including TB (35). Importantly, a recent clinical study clearly demonstrated that the booster vaccine, AERAS-402, induced polyfunctional $CD4^+$ T cells as well as a robust $CD8^+$ T-cell response in the circulation of human subjects (36). Likewise, longitudinal analysis of polyfunctional T-cell responses induced in peripheral blood by prime-boost immunization with AFRO-1 and AERAS-402 demonstrated that Mtb-specific proliferation and IFN-γ production was enhanced in rBCG/rAd35-vaccinated compared with BCG/rAd35-vaccinated or unvaccinated animals (13). Consistent with these published findings, our *in situ* observations in the same NHP cohort suggest that the induction of $CD8^+$ CTLs in Mtb-infected tissue was associated with polyfunctional post-vaccination T-cell responses detected in the circulation of the NHPs that were analyzed in this study (Table 1) (13).

$CD8^+$ T cells have been shown to be critical for the induction of protective TB immunity in humans (37), NHPs (38), rodents (39) and cattle (40). Of importance, CTLs are armed with granule-associated cytolytic and antimicrobial effector proteins, perforin and granulysin, which cooperate to eliminate infected macrophages and bacteria (5). *In vivo* cytolytic activity of $CD8^+$ T cells has been demonstrated in the lungs and lymphoid sites of Mtb-infected mice (41), and $CD8^+$ T cells lacking perforin possessed greatly reduced cytolytic capacity (4). Cytotoxicity of Mtb-specific pulmonary $CD8^+$ CTLs persisted for at least 37 wks after infection (41), confirming that CTL activity is stable during the course of chronic Mtb infection. Our findings illustrate that expression of $CD4^+$ T cells, in contrast to $CD8^+$ T cells, did not correlate with expression of $CD3^+$ T cells or the upregulation of perforin or granulysin in either lung lesions or spleen of rBCG-primed animals. $CD4^+$ T-cell numbers were comparable regardless of disease prognosis and thus could not be linked to an enhanced survival of Mtb-infected animals. It has been reported that $CD4^+$ Th1 cells are more important in the early, acute phase of Mtb infection, whereas $CD8^+$ CTLs have a prominent role during late stages of infection (42,43). Of interest, $CD4^+$ T cell–independent activation of highly cytolytic perforin-expressing $CD8^+$ T cells can also be induced by dendritic cells infected with live BCG (44).

To date, it has been difficult to find biomarkers to accurately monitor immune protection in TB and to evaluate new TB vaccine candidates, particularly markers that can be measured in easily accessible samples such as peripheral blood. Recently, it was shown that perforin and granulysin, but not IFN-γ, may be used as potential immune correlates after vaccination and Mtb challenge in bovine TB (45). The clinical relevance of granule-dependent CTL killing of mycobacteria-infected cells has been described in studies using tissue (6,7,46) or blood (47,48) obtained from patients with progressive TB disease. Of particular clinical importance, it was recently demonstrated that anti-TNF therapy in patients with autoimmune disorders, who have a greatly increased risk to develop active TB, selectively depleted perforin- and granulysin-expressing $CD8^+$ $CD45RA^+$ $CCR7^-$ effector memory T cells (T_{EMRA}), resulting in progression of TB disease (49). Accordingly, skewed maturation of Mtb-specific $CD8^+$ T cells in children with active TB was shifted toward a potent T_{EMRA} response and clinical recovery after successful chemotherapy (50). Pre-terminally differentiated $CD8^+$ T_{EMRA} cells (51) expressing low levels of perforin (52) have also been shown to be associated with progressive HIV infection. Homeostatic cytokines such as IL-7 and IL-15 promote the development of terminally differentiated and highly lytic human $CD8^+$ T_{EMRA} cells (53). IL-7 specifically enhances $CD8^+$ CTL activity by upregulating ser-

ine esterases (54) and perforin (55). In line with these findings, it was previously shown that *in vivo* administration of IL-7 or IL-15 (8) together with the BCG vaccine (56) prolonged survival of Mtb-infected mice. Protective immunity was associated with a relative increase in $CD8^+$ T cells compared with $CD4^+$ T cells (8), which is consistent with a high ratio of $CD8^+$ to $CD4^+$ T cells (3:1) in lung lesions from rBCG/rAd35-vaccinated animals. It is interesting that both IL-7 (26) and granulysin (46) were strongly upregulated in skin lesions of *Mycobacterium leprae*–infected patients with mild, but not severe, disease, which suggests that IL-7 may contribute to the quality of cell-mediated immune responses at the local site of mycobacterial infection.

Designing vaccines that mimic virulent TB strains, promoting phagolysosomal translocation into the cytosol (12), is likely critical to enhance $CD8^+$ T-cell activation by processing and presentation of cytosolic antigens via the MHC class I pathway. Cytosolic localization and replication of virulent mycobacteria are pathogenic features, causing apoptosis of infected macrophages (11,12), which may significantly improve cross-priming and subsequent T cell–mediated immunity (11,57). In this study, *in situ* protein levels as well as the survival of the BCG/rAd35-vaccinated animals were similar compared with the unvaccinated control NHPs, which may suggest that the prime vaccine must enable phagolysosomal escape of mycobacterial proteins in the cytosol to effectively trigger $CD8^+$ T cells and enhance immune protection. It has previously been shown that the BCG vaccine cannot protect rhesus macaques from developing progressive TB disease, whereas cynomolgus monkeys were almost completely protected by BCG (58). Interestingly, the immune response in animals with poor prognosis was associated with higher Mtb antigen load and an increased proportion of $CD68^+$ macrophages in the Mtb infected tissue, but also with a decreased CTL response. Deficient levels of perforin and granulysin expressing $CD8^+$ CTLs could result in reduced killing of Mtb-infected macrophages. Furthermore, macrophage activation and their T cell–activating properties may be decreased in susceptible animals, perhaps because of reduced levels of IL-7, which has been reported to augment monocyte effector functions (59). Instead, increased numbers of B cells may contribute to the formation of secondary lymphoid structures near pulmonary granulomas (60), which may enhance antigen presentation but also promote the induction of humoral immunity locally in the lung.

CONCLUSION

In summary, we provide evidence that the rBCG prototype strain AFRO-1 and the booster vaccine vector rAd35 AERAS-402 potentiates the expansion and/or accumulation of perforin- and granulysin-expressing $CD8^+$ T cells in the lung and lymphoid organs of Mtb-infected NHPs. Elevated CTL responses correlated with decreased Mtb antigen load in the tissue and with improved clinical outcome of rBCG/rAd35-vaccinated animals. These results support the development of TB vaccine concepts on the basis of priming of antimicrobial $CD8^+$ effector memory T cells and also the potential implementation of CTL correlates of immune protection in the assessment of vaccine-induced immune responses.

ACKNOWLEDGMENTS

We thank Sven Hoffner at the Department of Bacteriology and the personnel at the P3 safety laboratory, Swedish Institute for Infectious Disease Control, Sweden, for providing excellent laboratory facilities as well as technical support. We also thank Anette Hofmann at the Center for Infectious Medicine, Karolinska Institutet, Sweden, for assistance with confocal microscopy.

This work was supported by funding from the Aeras Global TB Vaccine Foundation (http://www.aeras.org/home/home.php), the Swedish Research Council, Vinnova, the Swedish Committee for International Health Care Collaboration, the Heart and Lung Foundation, the Swedish International Development Cooperation Agency and the von Kantzow Foundation.

DR Sizemore, CA Scanga, F Weichold and J Sadoff provided the vaccine constructs used in this study.

DISCLOSURE

The authors declare that they have no competing interests as defined by Molecular Medicine, or other interests that might be perceived to influence the results and discussion reported in this paper.

REFERENCES

1. Andersen P, Doherty TM. (2005) The success and failure of BCG: implications for a novel tuberculosis vaccine. *Nat. Rev.* 3:656–62.
2. Flynn JL, Chan J. (2001) Immunology of tuberculosis. *Annu. Rev. Immunol.* 19:93–129.
3. Stenger S, *et al.* (1997) Differential effects of cytolytic T cell subsets on intracellular infection. *Science.* 276:1684–7.
4. Woodworth JS, Wu Y, Behar SM. (2008) *Mycobacterium tuberculosis*-specific CD8+ T cells require perforin to kill target cells and provide protection in vivo. *J. Immunol.* 181:8595–603.
5. Stenger S, *et al.* (1998) An antimicrobial activity of cytolytic T cells mediated by granulysin. *Science.* 282:121–5.
6. Andersson J, Samarina A, Fink J, Rahman S, Grundstrom S. (2007) Impaired expression of perforin and granulysin in CD8+ T cells at the site of infection in human chronic pulmonary tuberculosis. *Infect. Immun.* 75:5210–22.
7. Rahman S, *et al.* (2009) Compartmentalization of immune responses in human tuberculosis: few CD8+ effector T cells but elevated levels of FoxP3+ regulatory T cells in the granulomatous lesions. *Am. J. Pathol.* 174:2211–24.
8. Maeurer MJ, *et al.* (2000) Interleukin-7 or interleukin-15 enhances survival of *Mycobacterium tuberculosis*-infected mice. *Infect. Immun.* 68:2962–70.
9. Skeiky YA, Sadoff JC. (2006) Advances in tuberculosis vaccine strategies. *Nat. Rev.* 4:469–76.
10. Sun R, *et al.* (2009) Novel recombinant BCG expressing perfringolysin O and the over-expression of key immunodominant antigens; preclinical characterization, safety and protection against challenge with *Mycobacterium tuberculosis*. *Vaccine.* 27:4412–23.
11. Grode L, *et al.* (2005) Increased vaccine efficacy against tuberculosis of recombinant *Mycobacterium bovis* bacille Calmette-Guerin mutants that secrete listeriolysin. *J. Clin. Invest.* 115:2472–9.
12. van der Wel N, *et al.* (2007) *M. tuberculosis* and *M. leprae* translocate from the phagolysosome to the cytosol in myeloid cells. *Cell.* 129:1287–98.
13. Magalhaes I, *et al.* (2008) rBCG induces strong antigen-specific T cell responses in rhesus macaques in a prime-boost setting with an aden-

ovirus 35 tuberculosis vaccine vector. *PloS One.* 3:e3790.
14. Bjork L, Andersson U, Chauvet JM, Skansen-Saphir U, Andersson J. (1994) Quantification of superantigen induced IFN-gamma production by computerised image analysis—inhibition of cytokine production and blast transformation by pooled human IgG. *J. Immunol. Methods.* 175:201–13.
15. Andersson J, *et al.* (1994) Concomitant in vivo production of 19 different cytokines in human tonsils. *Immunol.* 83:16–24.
16. Andersson J, *et al.* (1999) Perforin is not co-expressed with granzyme A within cytotoxic granules in CD8 T lymphocytes present in lymphoid tissue during chronic HIV infection. *AIDS (London, England)* 13:1295–303.
17. Agren K, *et al.* (1996) The production of immunoregulatory cytokines is localized to the extrafollicular area of human tonsils. *Acta Otolaryngol.* 116:477–85.
18. Behbahani H, *et al.* (2000) Normalization of immune activation in lymphoid tissue following highly active antiretroviral therapy. *J. Acquir. Immune Defic. Syndr.* 25:150–6.
19. Nilsson J, *et al.* (2006) HIV-1-driven regulatory T-cell accumulation in lymphoid tissues is associated with disease progression in HIV/AIDS. *Blood.* 108:3808–17.
20. Soderlund J, *et al.* (2004) Dichotomy between CD1a+ and CD83+ dendritic cells in lymph nodes during SIV infection of macaques. *J. Med. Primatol.* 33:16–24.
21. Westermann J, Pabst R. (1992) Distribution of lymphocyte subsets and natural killer cells in the human body. *Clin. Invest.* 70:539–44.
22. Havenga M, *et al.* (2006) Novel replication-incompetent adenoviral B-group vectors: high vector stability and yield in PER.C6 cells. *J. Gen. Virol.* 87:2135–43.
23. Madri JA, Furthmayr H. (1980) Collagen polymorphism in the lung: an immunochemical study of pulmonary fibrosis. *Hum. Pathol.* 11:353–66.
24. Baba K, *et al.* (2008) Rapid and specific diagnosis of tuberculous pleuritis with immunohistochemistry by detecting *Mycobacterium tuberculosis* complex specific antigen MPT64 in patients from a HIV endemic area. *Appl. Immunohistochem. Mol. Morphol.* 16:554–61.
25. Wang Z, *et al.* (2007) The solution structure of antigen MPT64 from *Mycobacterium tuberculosis* defines a new family of beta-grasp proteins. *J. Mol. Biol.* 366:375–81.
26. Sieling PA, *et al.* (1995) IL-7 in the cell-mediated immune response to a human pathogen. *J. Immunol.* 154:2775–83.
27. Wilkinson KA, *et al.* (2005) Ex vivo characterization of early secretory antigenic target 6-specific T cells at sites of active disease in pleural tuberculosis. *Clin. Infect. Dis.* 40:184–7.
28. Barnes PF, *et al.* (1989) Compartmentalization of a CD4+ T lymphocyte subpopulation in tuberculous pleuritis. *J. Immunol.* 142:1114–9.
29. Jafari C, *et al.* (2008) Local immunodiagnosis of pulmonary tuberculosis by enzyme-linked immunospot. *Eur. Respir. J.* 31:261–5.
30. Schwander SK, *et al.* (1998) Enhanced responses to *Mycobacterium tuberculosis* antigens by human alveolar lymphocytes during active pulmonary tuberculosis. *J. Infect. Dis.* 178:1434–45.
31. Nemeth J, *et al.* (2009) Recruitment of *Mycobacterium tuberculosis* specific CD4+ T cells to the site of infection for diagnosis of active tuberculosis. *J. Intern. Med.* 265:163–8.
32. Lurquin C, *et al.* (2005) Contrasting frequencies of antitumor and anti-vaccine T cells in metastases of a melanoma patient vaccinated with a MAGE tumor antigen. *J. Exp. Med.* 201:249–57.
33. McElrath MJ, *et al.* (2008) HIV-1 vaccine-induced immunity in the test-of-concept Step Study: a case-cohort analysis. *Lancet.* 372:1894–905.
34. Darrah PA, *et al.* (2007) Multifunctional TH1 cells define a correlate of vaccine-mediated protection against *Leishmania major*. *Nat. Med.* 13:843–50.
35. Forbes EK, *et al.* (2008) Multifunctional, high-level cytokine-producing Th1 cells in the lung, but not spleen, correlate with protection against *Mycobacterium tuberculosis* aerosol challenge in mice. *J. Immunol.* 181:4955–64.
36. Abel B, *et al.* (2010) The novel tuberculosis vaccine, AERAS-402, induces robust and polyfunctional CD4+ and CD8+ T cells in adults. *Am. J. Respir. Crit. Care Med.* 181:1407–17.
37. Smith SM, *et al.* (1999) Characterization of human *Mycobacterium bovis* bacille Calmette-Guerin-reactive CD8+ T cells. *Infect. Immun.* 67:5223–30.
38. Chen CY, *et al.* (2009) A critical role for CD8 T cells in a nonhuman primate model of tuberculosis. *PLoS Pathog.* 5:e1000392.
39. Flynn JL, Goldstein MM, Triebold KJ, Koller B, Bloom BR. (1992) Major histocompatibility complex class I-restricted T cells are required for resistance to *Mycobacterium tuberculosis* infection. *Proc. Natl. Acad. Sci. U. S. A.* 89:12013–7.
40. Hogg AE, Worth A, Beverley P, Howard CJ, Villarreal-Ramos B. (2009) The antigen-specific memory CD8+ T-cell response induced by BCG in cattle resides in the CD8+gamma/deltaTCR-CD45RO+ T-cell population. *Vaccine.* 27:270–9.
41. Kamath AB, *et al.* (2004) Cytolytic CD8+ T cells recognizing CFP10 are recruited to the lung after *Mycobacterium tuberculosis* infection. *J. Exp. Med.* 200:1479–89.
42. van Pinxteren LA, Cassidy JP, Smedegaard BH, Agger EM, Andersen P. (2000) Control of latent *Mycobacterium tuberculosis* infection is dependent on CD8 T cells. *Eur. J. Immunol.* 30:3689–98.
43. Laochumroonvorapong P, *et al.* (1997) Perforin, a cytotoxic molecule which mediates cell necrosis, is not required for the early control of mycobacterial infection in mice. *Infect. Immun.* 65:127–32.
44. Tsunetsugu-Yokota Y, *et al.* (2002) Selective expansion of perforin-positive CD8+ T cells by immature dendritic cells infected with live Bacillus Calmette-Guerin mycobacteria. *J. Leukoc. Biol.* 72:115–24.
45. Capinos Scherer CF, *et al.* (2009) Evaluation of granulysin and perforin as candidate biomarkers for protection following vaccination with *Mycobacterium bovis* BCG or M. bovisDeltaRD1. *Transbound. Emerg. Dis.* 56:228–39.
46. Ochoa MT, *et al.* (2001) T-cell release of granulysin contributes to host defense in leprosy. *Nat. Med.* 7:174–9.
47. Dieli F, *et al.* (2001) Granulysin-dependent killing of intracellular and extracellular *Mycobacterium tuberculosis* by Vgamma9/Vdelta2 T lymphocytes. *J. Infect. Dis.* 184:1082–5.
48. Sahiratmadja E, *et al.* (2007) Plasma granulysin levels and cellular interferon-gamma production correlate with curative host responses in tuberculosis, while plasma interferon-gamma levels correlate with tuberculosis disease activity in adults. *Tuberculosis.* 87:312–21.
49. Bruns H, *et al.* (2009) Anti-TNF immunotherapy reduces CD8+ T cell-mediated antimicrobial activity against *Mycobacterium tuberculosis* in humans. *J. Clin. Invest.* 119:1167–77.
50. Caccamo N, *et al.* (2006) Phenotypical and functional analysis of memory and effector human CD8 T cells specific for mycobacterial antigens. *J. Immunol.* 177:1780–5.
51. Champagne P, *et al.* (2001) Skewed maturation of memory HIV-specific CD8 T lymphocytes. *Nature.* 410:106–11.
52. Appay V, *et al.* (2000) HIV-specific CD8(+) T cells produce antiviral cytokines but are impaired in cytolytic function. *J. Exp. Med.* 192:63–75.
53. Geginat J, Lanzavecchia A, Sallusto F. (2003) Proliferation and differentiation potential of human CD8+ memory T-cell subsets in response to antigen or homeostatic cytokines. *Blood.* 101:4260–6.
54. Hickman CJ, Crim JA, Mostowski HS, Siegel JP. (1990) Regulation of human cytotoxic T lymphocyte development by IL-7. *J. Immunol.* 145:2415–20.
55. Smyth MJ, Norihisa Y, Gerard JR, Young HA, Ortaldo JR. (1991) IL-7 regulation of cytotoxic lymphocytes: pore-forming protein gene expression, interferon-gamma production, and cytotoxicity of human peripheral blood lymphocytes subsets. *Cell. Immunol.* 138:390–403.
56. Singh V, *et al.* (2010) Coadministration of interleukins 7 and 15 with Bacille Calmette-Guerin mounts enduring T cell memory response against *Mycobacterium tuberculosis*. *J. Infect. Dis.* 202:480–9.
57. Schaible UE, *et al.* (2003) Apoptosis facilitates antigen presentation to T lymphocytes through MHC-I and CD1 in tuberculosis. *Nat. Med.* 9:1039–46.
58. Langermans JA, Andersen P, van Soolingen D, *et al.* (2001) Divergent effect of bacillus Calmette-Guerin (BCG) vaccination on *Mycobacterium tuberculosis* infection in highly related macaque species: implications for primate models in tuberculosis vaccine research. *Proc. Natl. Acad. Sci. U S A.* 98:11497–502.
59. Gessner A, Vieth M, Will A, Schroppel K, Rollinghoff M. (1993) Interleukin-7 enhances antimicrobial activity against *Leishmania major* in murine macrophages. *Infect. Immun.* 61:4008–12.
60. Ulrichs T, *et al.* (2004) Human tuberculous granulomas induce peripheral lymphoid follicle-like structures to orchestrate local host defence in the lung. *J. Pathol.* 204:217–28.